Colloid Polym Sci 277:658–665 (1999)

ORIGINAL CONTRIBUTION

Y-M. Wang
C.Y. Pan

Study of the mechanism of the emulsifier-free emulsion polymerization of the styrene/4-vinylpyridine system

Received: 9 September 1998
Accepted in revised form: 23 February 1999

Y-M. Wang (✉) · C.Y. Pan
Department of Polymer Science
and Engineering
University of Science and Technology
of China
Hefei 230026, China
e-mail: pcy@ustc.edu.cn
Fax: +86-0551-3633760

Abstract For the emulsifier-free emulsion copolymerization of styrene with the water-soluble comonomer 4-vinylpyrindine (4VP), and using ammonium persulfate as an initiator, the kinetics, the content of 4VP, the molecular weight and the molecular weight distributions of the polymer at various conversions, and particle morphologies have been investigated. Based on the results obtained, the particle nucleation mechanism was discussed.

Key words Emulsifier-free emulsion polymerization – Oligomeric emulsifier – Oligomeric particles – Oligomeric emulsifier reservoir – Micelle nucleation

Introduction

Emulsifier-free emulsion polymerization has been extensively used to prepare particles with functional groups on their surfaces for biomedical and catalytic support applications, and to synthesize latexes without surfactant migration after film formation for coating and adhesive applications. In such polymerization systems, polymer particles are stabilized by the polymer capped with hydrophilic groups produced by ionizable initiators, such as potassium persulfate [1, 2], or by ionic polymers prepared by adding comonomers with ionic groups, such as carboxylic monomers [3, 4], sodium sulfoethyl methacrylate [5], and sodium styrene sulfonate [5], and sodium undecylenic isethionate [6] etc., to the polymerization system, and some nonionic monomers, such as glycidyl methacrylate [7] and 2-hydroxyethyl methacrylate, [8] were also used as comonomers for stabilizing the particles. Several mechanisms for particle nucleation and growth in emulsion polymerization without emulsifier have been proposed based upon the water solubility of the monomers. For example, in the presence of the water-soluble initiator potassium persulfate (KPS) slightly water-soluble monomers, such as styrene (St), were initiated and polymerized in the aqueous phase to produce oligomer radicals with end sulfate groups, followed by micelle formation [1]. However, for more water-soluble monomers, such as methacrylates [9, 10], the growing chains were precipitated to form particles until the chain length reached to a critical value, which varied with monomers such as this values of methyl methacrylate is 60–80. In both cases, subsequent polymerization occurred in monomer swollen particles. In recent years, a theory of coagulate nucleation of precursor particles was proposed: it said that the stable latex was formed from the coagulation and growth of unstable precursor particles formed through homogenous nucleation. The rate of particle formation was determined by the rate of homogeneous nucleation to form primary precursors, the rate of coagulation of precursor particles, and the rate of propagation growth [11].

With regard to the nucleation mechanism for the emulsifier-free system of St and 4-vinylpyridine (4VP), only very few studies have been reported [12]. In our previous work [13], the effects of 4VP content in the St–4VP system on the formation of the particles were investigated, but the kinetics of the formation has not been studied in detail. Thus, we report our studies on the kinetics and the mechanism of emulsifier-free emulsion polymerization of poly(St-*co*-4VP) [(P(St-*co*-4VP)].

Experimental

Materials

St (CR, Central Chemical Plant of Shanghai Chemical Reagent Station) was distilled at 40 °C/14.5 mmHg and stored at 4 °C. 4VP (Merck-Schuchardt, Munich) was distilled at 55 °C/18 mmHg before use. Ammonium persulfate (APS, Anjian Chemical Plant of Shanghai) was analytical grade and was used without further purification.

Emulsion polymerization

A typical recipe for the preparation of the St-*co*-4VP copolymer latex is listed in Table 1. The polymerization was carried out at 70 °C, and with a stirrer speed of 350 rpm under a nitrogen atmosphere. All the ingredients except the APS solution were placed in a 500 ml four-neck round-bottom flask equipped with a mechanical stirrer, a reflux condenser, a thermometer, a nitrogen inlet tube, and a feeding funnel. The reaction system was purged with nitrogen for 1 h prior to the addition of the APS solution.

Measurement and characterization

The samples withdrawn from the reaction solution were quenched in ice–water, then vacuum–dried at room temperature until the weight of the sample remained constant. Whether the inhibitor, hydroquinone, was added to the samples or not, the results were the same. The total conversions of St and 4VP were calculated according to Eq. (1):

$$C(\%) = \frac{W_1/W_2}{m_1/(m_1+m_2)} \times 100\% \ , \tag{1}$$

where C is the total conversion of polymer, W_1 is the weight of dried polymer, W_2 is the weight of the sample withdrawn from the reaction solution, m_1 is the weight of total monomer, and m_2 is the weight of the medium.

The size and morphology of the P(St-*co*-4VP) microspheres were investigated by transmission electron microscopy (TEM) (H-80C microscope) and the weight-average diameter (d) was calculated based on $\sum n_i d_i^3 / \sum n_i d_i^2$, where n_i is the number of particles with diameter d_i. The latex particle size distribution was calculated based on the sizes of about 100 particles on different regions of the TEM photographs. The number of latex particles (N) per unit volume of aqueous medium was calculated based on Eq. (2):

$$N = \frac{6CW}{\pi d^3 DV} \ , \tag{2}$$

where C, W, D, and V are the conversion, the total weight of monomers added, the average density of the copolymer obtained, and the volume of the aqueous medium. The number, the weight-average molecular weights and the molecular weight distribution were measured on a Waters 150C gel-permeation chromatography (GPC) with ultrastyragel columns (Waters Co.) in series having a molecular weight exclusion limit from 500 to 10^5 at 1.5 ml/min, using tetrahydrofuran (THF) as the solvent (whether the *N*,*N*,*N*′,*N*′-tetramethylethylemediamine was added to the THF or not, the results were the same) and PSt as the standard. The content of 4VP (X_p) in the polymer particles was determined by the following procedure. The solid samples after determination of the degree of conversion were dissolved in $CDCl_3$, an amount of CH_2Cl_2 was added into the solution as a standard, then it was measured on a DMX-500 NMR instrument, and the weight fraction of 4VP in the polymer particles was calculated using Eq. (3):

$$X_\mathrm{p} = \frac{aS_2M}{S_1W} \ , \tag{3}$$

in which a is the number of moles of CH_2Cl_2 added to the sample, S_2 is the integral value of the peak at $\delta = 8.15$ ppm, corresponding to the two protons near the nitrogen of 4VP, S_1 is the integral value of the peak at $\delta = 5.2$ ppm, representing the two protons of CH_2Cl_2, M is the molecular weight of 4VP, and W is the weight of the polymer.

Table 1 Recipes for the emulsifier-free emulsion polymerization of polylstyrene-*co*-4-vinylpyrindine [P(St-*co*-4VP)] latex

Compound	St	4VP	Ammonium persulfate	H_2O
Amount (g)	36.00	6.00	0.122	398

Results and discussion

Conversion

The curve of conversion versus time shown in Fig. 1 is concave upward until about 90% conversion, after which the curve suddenly levels off and the conversion increases slightly with time. Three intervals (I, II, III) can be observed from the curve of the polymerization rate versus conversion (Fig. 2). The polymerization rate increased with conversion in interval I, then became constant near 10% conversion (Fig. 2), indicating that the nucleation period had ended. The maximum in interval I (curve from A to B in Fig. 2) is probably attributed to a transient high particle number, which was confirmed by the abrupt decrease in particle number near 10% conversion (Fig. 3). The curve of particle number versus conversion in this region in Fig. 3 will be explained later. During interval II, the polymerization rate is constant (Fig. 2, behavior C) for the same reason as in conventional emulsion polymerization, and then increases with conversion (curve from C to D in Fig. 2) which is a consequence of the gel effect. The polymer particles increased greatly in size while the monomer

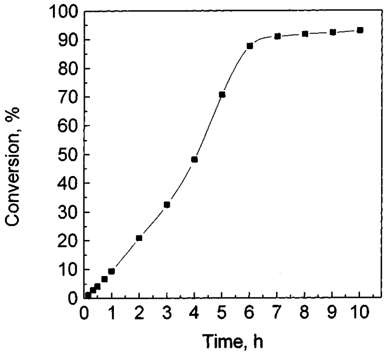

Fig. 1 Degree of conversion versus time

droplets decreased in size (Fig. 4). The polymerization rate decreased abruptly near 90% conversion, indicating the end of interval II and the disappearance of the monomer droplets, although the particle number in interval III remained the same as in interval II (Fig. 3). The monomer concentration in the particles decreased with conversion and monomer droplets were no longer present, therefore, the polymerization rate decreased with the conversion in interval III.

The three intervals observed are the same as in conventional emulsion polymerization. The only difference was the low polymerization rate in interval I, because time was needed to produce the stabilizer of the particles; therefore, the mechanism of nucleation of emulsion emulsifier-free polymerization would be different from conventional emulsion polymerization. This will be discussed latter.

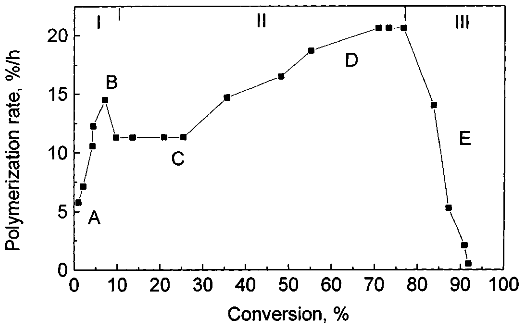

Fig. 2 Polymerization rate versus degree of conversion

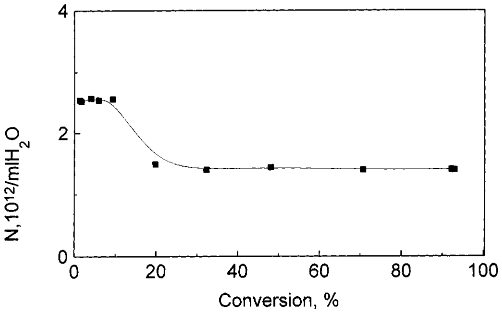

Fig. 3 Particle number density (*N*) versus degree of conversion

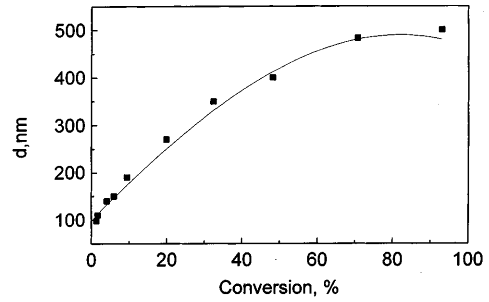

Fig. 4 Particle diameter (*d*) versus degree of conversion

Content of 4VP in the polymer

The 4VP content of the copolymer at various conversions was calculated according to Eq. (3). The results are shown in Fig. 5. In early stages (below a conversion of 4.10%), the copolymers capped with sulfonic acid groups contained more than 40 wt% 4VP (Fig. 5), and were insoluble in $CHCl_3$, THF etc., thus, the exact contents could not be calculated based on NMR data, but were obtained from elementary analysis of the samples. This fact infers that the particles observed in Fig. 8a–c mainly consisted of oligomers rich in 4VP, and that they act as a reservoir providing emulsifier. The instantaneous 4VP content of the copolymer (A_{VP}) obtained at each conversion can be calculated according to Eq. (4).

$$A_{VP}(\mathrm{wt\%}) = \frac{[(X_p)_{t_2}C_{t_2} - (X_p)_{t_1}C_{t_1}]}{C_{t_2} - C_{t_1}} \times 100\% \ , \qquad (4)$$

where C_{t_2} and C_{t_1} are the conversions at t_2 and t_1, and $(X_p)_{t_2}$ and $(X_p)_{t_1}$ are the 4VP contents of the copolymers obtained at t_2 and t_1, respectively. The results are shown in Fig. 6. Generally, the copolymer produced from the copolymerization in the aqueous phase contained a higher content of 4VP because of the high solubility of 4VP in water. The abrupt decrease in the instantaneous 4VP content in the copolymer at around 10 wt% conversion as shown in Fig. 6 demonstrated the end of polymerization in the aqueous phase, and then the polymerization occurred completely in micelles or in polymer particles. The instantaneous composition of the copolymer should be determined by the relative concentration of St and 4VP in the micelles or in the polymer particles, which in turn is controlled by the diffusion rate of monomers from the water phase. When the ratio of St

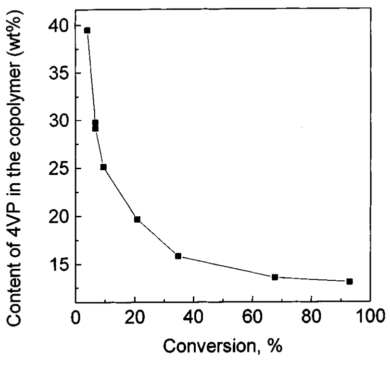

Fig. 5 The relationship between the content of 4-vinylpyridine (4*VP*) in the copolymer and the degree of conversion

to 4VP was set up, the content of 4VP in the copolymer remained constant. This is observed in Fig. 6 after around 10 wt% conversion.

Molecular weight and molecular weight distribution

GPC curves of the samples at various degrees of conversion are shown in Fig. 7. When the conversion was below 4.1%, the solubility of the samples in THF was too poor to measure their GPC curves. A bimodel molecular weight distribution, one distribution centered at a number molecular weight of 10^4, the other at 2000, was observed below 50% conversion (Fig. 7). The shift of the higher molecular weight peak to much higher molecular weights was negligible below 10%. As the polymerization proceeds further, the major peak shifts gradually to the higher molecular weight region and the oligomeric peak disappears. This phenomenon was also observed in the St/KPS/water system [1].

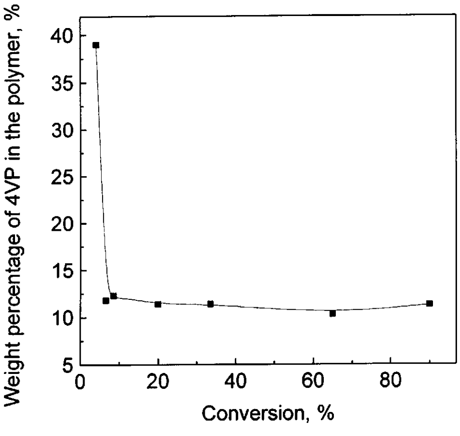

Fig. 6 Instantaneous weight percentages of 4VP in the copolymer at different degrees of conversion

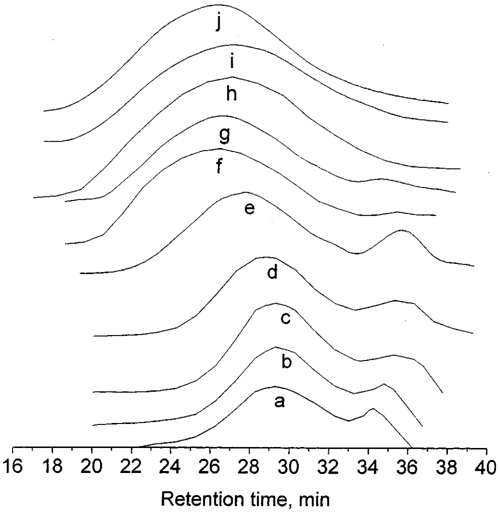

Fig. 7 Molecular weight distribution at different degrees of conversion (*a*) 30 min, 4.1%; (*b*) 45 min, 6.7%; (*c*) 60 min, 9.4%; (*d*) 120 min, 20.9%; (*e*) 180 min, 32.4%; (*f*) 240 min, 48.1%; (*g*) 300 min, 70.7%; (*h*) 360 min, 87.6%; (*i*) 420 min, 90.9%; (*j*) 600 min, 93.0%

Particle morphology

TEM micrographs of the polymer particles at various conversions are shown in Fig. 8. The particles at the earlier stage (at 1.3% conversion) have an anomalous shape with an uneven surface, (Fig. 8a). This is probably caused by the absorption of a considerable amount of water, because the particles consisted of the oligomer rich in 4VP. While drying the latex on the copper grid for TEM observation, the particles exhibited an anomalous shape with an uneven surface.

At 2.8% conversion, some of the particles had the morphology of a sphere with an empty core (Fig. 8b). This morphology was also found in the St/KPS/water systems [1]. The empty core morphology resulted from a flash evaporation of the St in the small particles during dynamic vacuum pumping. This is evidence that the monomer droplets formed were stabilized by the copolymer rich in 4VP.

At 4.1% conversion, the number of particles having an empty core decreased. When the polymerization proceeded further, the particles became spherical as shown in Fig. 8d–f. This is due to the decrease in the number of 4VP units relative to the number of St units in the particles.

Particle nucleation mechanism

When the conversion was less than 4.1%, the oligomers contained 40 wt% 4VP, were insoluble in THF, and GPC measurements could not be carried out. When the conversion was higher than 4.1%, a bimodel molecular weight distribution was observed, indicating that two polymerization mechanisms existed. In order to understand these phonomena, samples taken from the system at 20, 30, 180, and 600 min were subjected to the following treatment. The samples were centrifuged at 15 000 rpm for 30 min, and the particles in the latex solution were precipitated. The clear solution above the precipitates was removed and then dried under vacuum. The polymers or oligomers in the particle phase (the precipitates) and in the aqueous phase were both subjected to molecular weight distribution measurements and elemental analysis of nitrogen. The results are shown in Table 2. When polymerization was carried out for 20 min, the particles were insoluble in THF, and mainly consisted of oligomers containing sulfate and pyridine groups. Thus it is reasonable that most of the

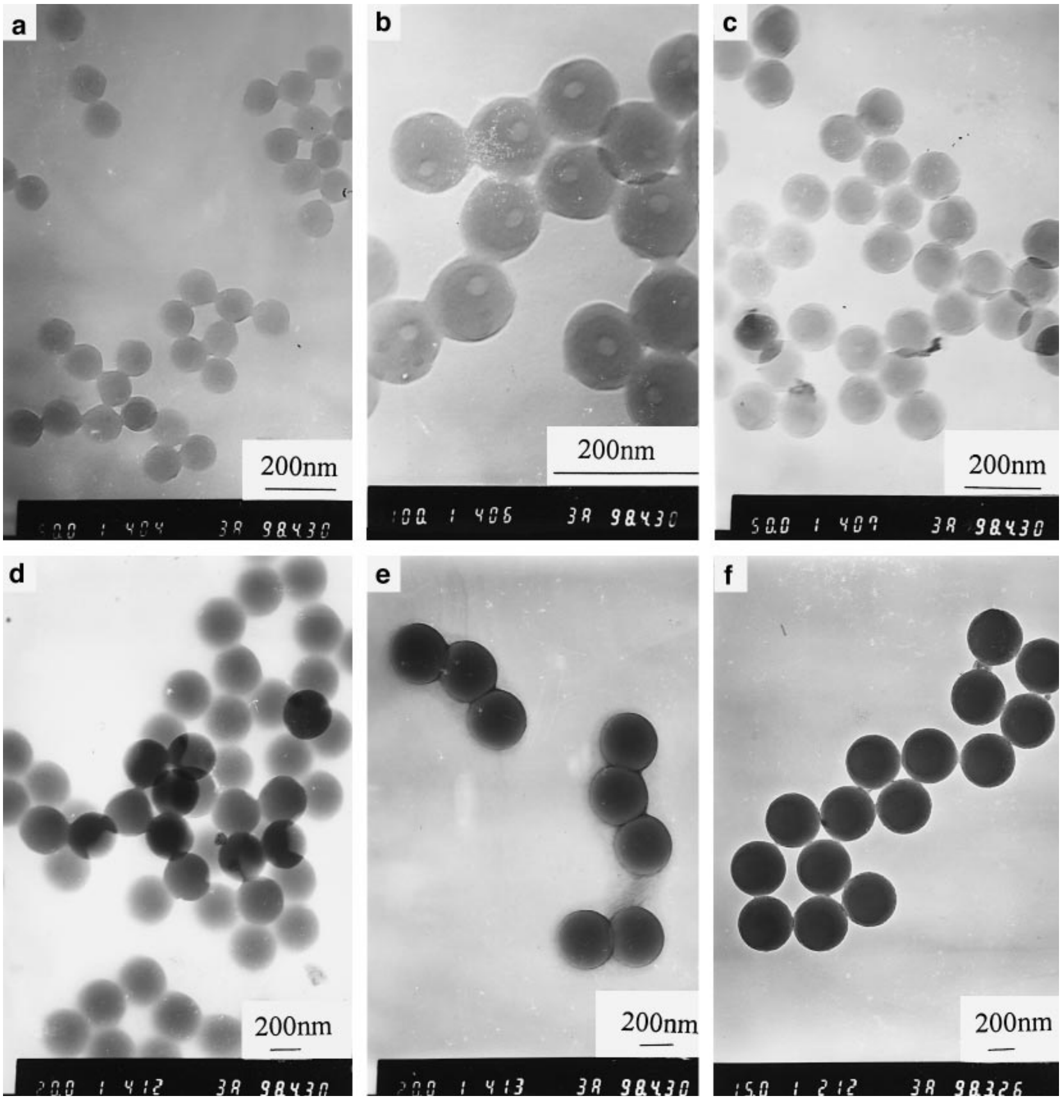

Fig. 8a–f Transmission electron microscopy micrographs of polymer particles at different stages of polymerization for styrene (*St*) and 4VP. **a** 10 min, 1.3% conversion; **b** 20 min, 2.8%; **c** 30 min, 4.1%; **d** 180 min, 32.4%; **e** 240 min, 48.1%; **f** 600 min, 93.0%

particles represented in Fig. 8b are the result of oligomer aggregation. The polymers or/and the oliogomers in the aqueous phase were divided into two types: one was insoluble in THF, the other was soluble. The type insoluble in THF is an oligomer with a sulfate group and a high content of pyridine. The type soluble in THF is the polymer. As the polymerization proceeded the relative quantities of polymers and oligomers in the aqueous phase compared to the particles decreased, indicating that the polymerization occurred in micelles to form the particles and they grew in size. Based on the previous discussion the following mechanism for the particle formation is proposed. At the beginning of the polymerization, APS is thermally decomposed into primary radicals to induce the copolymerization of St and 4VP in the aqueous phase and the oligomers formed which were rich in the hydrophilic segment of 4VP acted as an emulsifier. They dissolved in the aqueous phase at first, when the concentration of oligomeric emulsifier exceeded its critical micelle concentration (cmc), the excess oligomer aggregated together to form micelles, and stabilized the monomer droplets. When the amount of oligomer formed was large enough (around 5 wt% in this case), the oligomers produced were precipitated and aggregated to form the particles, which are referred to as the oligomeric emulsifier reservoir. The monomers swollen in the micelles polymerized to form polymer particles. A simplified schematic representation of the emulsion polymerization process is shown in Fig. 9. In stage I, more and more oligomer emulsifier is formed by the copolymerization of St and 4VP in aqueous solution.

Table 2 Weight fraction of the polymer composition

Sample[a]	Time (min)	$M_n(10^4)$	$M_w(10^4)$	*D*	Relative weight of the polymer or oligomers in water to total polymer (wt%)	Relative weight of oligomers soluble in water to total oligomers (wt%)	Nitrogen content in the copolymer (wt%)
^{1}ws	20	4.01	5.95	1.48	0.35		6.01
^{1}w$_i$	20				1.75		10.51
^{2}ws	30	5.59	6.63	1.18	0.2		3.41
^{2}w$_i$	30				1.05	12.26	8.77
^{3}ws	180	4.68	5.82	1.24	0.02		1.56
^{3}w$_i$	180				0.1	0.8	5.60
^{4}ws	600	2.49	4.46	1.79	0.02		1.49
^{4}w$_i$	600						
^{1}p	20						3.94
^{2}p	30	3.93	14.17	3.6			3.43
^{3}p	180	2.28	7.26	3.18			1.78
^{4}p	600	2.03	5.75	2.84			1.62

[a] w and p represent the polymers formed in water and in the particles respectively. s and i represent the polymer soluble and insoluble in THF, respectively

The emulsifier molecules are dissolved in water as molecules, micelles, stabilized monomer droplets, and also formed particles stabilized by themselves. The copolymerization was carried out in micelles. That there was no polymer in the particles after 20 min is evidence that polymerization in oligomeric particles was negligible. Therefore, we can conclude that the particles were formed mainly from polymerization in micelles. Before the end of stage I, the formation of oligomer emulsifier ends. The lower content of nitrogen and the high molecular weight ($M_n = 4.01 \times 10^4$, see Table 2) of the polymer in water are evidence that the polymer was formed from polymerization in micelles. The system consists of three types of particles: monomer droplets, oligomeric emulsifier particles having the function of providing emulsifier, and active polymer particles where polymerization occurred. As the polymer particles grew in size, they absorbed more and more oligomers (in order to maintain stability) from solution, the oligomer concentration of which was maintained at the cmc level by dissolution of oligomers from the emulsifier reservoir. The point is quickly reached at which the emulsifier concentration in water fell below its cmc, the emulsifier reservoirs became smaller, and very early in interval II the emulsifier particles disappeared, which can be confirmed by the evidence that the number of particles at 20% conversion obtained from TEM observation did not reach a constant level as shown in Fig. 3, but the polymerization rate started to become constant at around 10% conversion (Fig. 2). The predicted maximum in the curve shown in Fig. 2 (curve AB) probably arose from high proportion of particles containing radicals. When the emulsion polymerization system was established, the polymerization progress was similar to conventional emulsion polymerization. In stage II, monomer from the monomer droplets diffused into the polymer particles, and polymerized. The size of the polymer particles increased with the decrease in the monomer droplet concentration, then the gel effect led to an increase in the polymerization rate. In interval III, the polymerization rate decreased due to the disappearance of the monomer droplets in the system.

The results listed in Table 2 demonstrate the very interesting phenomenon that the molecular weight of the polymer in the aqueous phase increased as polymerization proceeded during stage I, then decreased. The reason for this fact is probably that during stage I, primary radicals produced from the initiator initiated St and 4VP in the aqueous phase to polymerize. The copolymer formed (rich in 4VP) had the functions of an emulsifier and, at the same time, diffused to micelles or particles and initiated the monomers in micelles or particles to polymerize; thus, more micelles became polymer particles. Some particles were so small and could not be separated by centrifugation. We call these particles soluble particles. As the number of micelles and polymer particles increased, the life time of a radical in the soluble particles lengthend, and thus the molecular weight increased. After stage I, the polymerization of St and 4VP to form oligomers ended. All efficient primary radicals diffused into the polymer particles, and the molecular weight decreased because some of the oligomers were soluble in the aqueous phase.

Conclusions

Kinetics studies of emulsifier-free emulsion polymerization demonstrate three stages of the polymerization: the

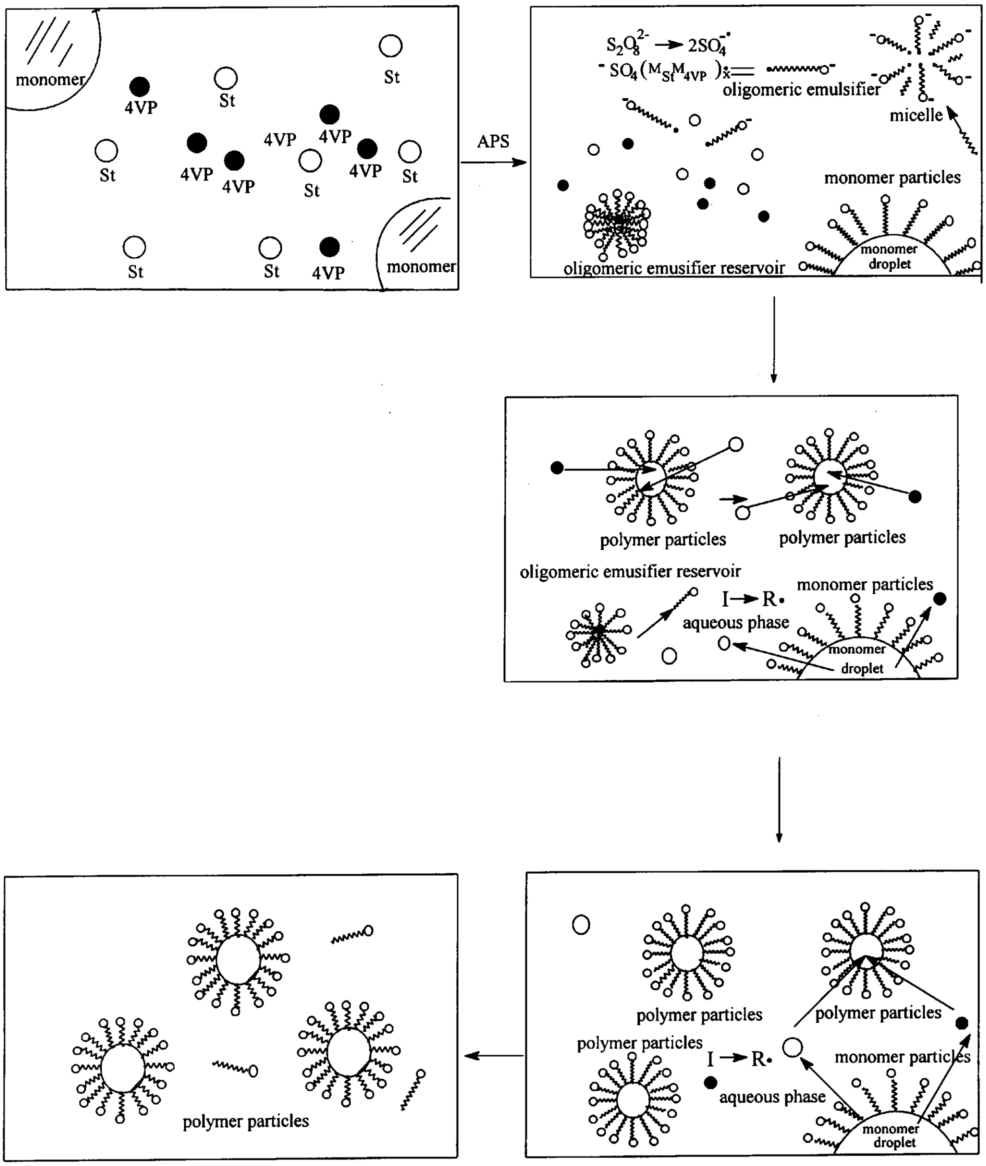

Fig. 9 Mechanism of particle formation for emulsifier-free emulsion polymerization of the St/4VP/ammonium persulfate system

end of stage I at conversion of around 10%, stage II at conversion of about 85% and then the beginning of stage III. Copolymerization of St and 4VP in the aqueous phase to form oligomers rich in the 4VP unit occurred. The oligomers capped with sulfate group and having pyridine groups act as emulsifiers and form micelle particles, stabilizing the monomer droplets. The polymer particles are formed via a micellization-type mechanism. During stage I, as the number of micelles and smaller polymer particles increases, the molecular weight of the polymer increases, because primary radicals initiates polymerization of the monomers in micelles and/or smaller polymer particles. The oligomer particles act as an emulsifier reservoir, and all disappear early in stage II. During stage II, the acceleration of polymerization due to the gel effect was observed. During stage III, the polymerization rate decreases rapidly.

References

1. Goodall AR, Wilkinson MC, Hearn J (1977) J Polym Sci Poly Chem Ed 15: 2193
2. Goodwin JW, Hearn Ho CC, Ottewill RH (1973) Br Polym J 5:347
3. Ceska GW (1973) J Appl Polym Sci 18: 2493
4. Sakota K, Okaya T (1976) J Appl Polym Sci 20:1725
5. Juang MS, Krieger IM (1976) J Polym Sci Polym Chem Ed 14:2089
6. Chen SA, Chang HS (1985) J Polym Sci Polym Chem Ed 23:2615
7. Zurkova E, Bouchal K, Zdenkova D, Pelzbauer Z, Svec F, Kalal J (1983) J Polym Sci Polym Chem Ed 21:2949
8. Kamei S, Okubo M, Matsumoto T (1986) J Polym Sci Polym Chem Ed 24: 3109
9. Fich RM, Prenosil MP, Sprick KJ (1969) J Polym Sci Part C 27:95
10. Arai M, Arai K, Saito S (1979) J Polym Sci Polym Chem Ed 17:3655
11. Feeney PJ, Napper DH, Gilbert RG (1987) Macromolecules 26:2922
12. Ohtsuka Y, Kawaguch H, Hayashi S (1981) Polymer 22:6258
13. Wang YM, Feng LX, Pan CY (1998) J Appl Polym Sci 70:2307